Progr Colloid Polym Sci (2004) 128: 21–24
DOI 10.1007/b97068

Claudio L.A. Berli
María V. Piaggio
Julio A. Deiber

Theoretical relation between the tube zeta potential and the background electrolyte composition in capillary electrophoresis

C.L.A. Berli · Julio A. Deiber (✉)
Instituto de Desarrollo Tecnológico para la Industria Química, Universidad Nacional del Litoral, Consejo Nacional de Investigaciones Científicas y Técnicas, Güemes 3450, 3000 Santa Fe, Argentina
e-mail: treoflu@ceride.gov.ar
Tel.: +54-342-4559174
Fax: +54-342-4550944

C.L.A. Berli
Departamento de Física, Facultad de Bioquímica y Ciencias Biológicas, Universidad Nacional del Litoral, Pje. El Pozo, 3000 Santa Fe, Argentina

M.V. Piaggio
Cátedra de Bioquímica Básica de Macromoléculas, FBCB, Universidad Nacional del Litoral, Pje. El Pozo, 3000 Santa Fe, Argentina

Abstract This work presents a theoretical analysis of the relation between the tube zeta potential and the electrolyte solution composition typically found in capillary electrophoresis. A model including the relevant physicochemical parameters of the capillary–solution interface is derived in the framework of Poisson–Boltzmann theory and is then validated experimentally. This model is applied to capillaries containing acidic groups attached to the inner wall as the main source of surface charges. In particular, experimental data of electroosmotic flow in synthetic organic polymer capillaries are considered to prove the validity of the model with less conventional solid materials. It is also found that the model describes successfully experimental data of the zeta potential for a wide range of pH and ionic strength.

Keywords Organic polymer capillaries · Electroosmotic flow · Capillary electrophoresis Zeta potential · Surface potential

Introduction

When an electrical field is applied along the axial direction of a capillary tube filled with an electrolyte solution, the so-called electroosmotic flow (EOF) develops [1–4]. This phenomenon is a manifestation of the presence of electrical charges on the inner capillary surface and the associated double layer of ions in solution. The electroosmotic fluid velocity v_{EO} is given by the Helmholtz–Smoluchowski equation, provided the relevant conditions are satisfied [5–7]. It is expressed

$$v_{EO} \approx -(\varepsilon/\mu)E\zeta, \quad (1)$$

where ε is the electrical permittivity, μ is the solution viscosity, E is the axial electrical field strength and ζ is the zeta potential at a moving boundary between the capillary wall and the solution. The EOF has critical implications in electrophoresis, mainly in capillary zone electrophoresis (CZE) [8–11], where the tubes used normally contain acidic groups attached to the wall as a source of surface charges. The resulting ζ is thus related to the chemical composition of the background electrolyte (BGE). Therefore, a rational formulation of solutions concerning pH, ionic strength, viscosity and electrical permittivity is required to optimize the separation performance of this technique [12–16]. Further, the knowledge of ζ is of particular interest in simulations of CZE, where "virtual electropherograms" are predicted from physicochemical data of the capillary, the BGE and analytes under separation [17–20].

In this context of analysis, one may observe that theoretical work is required to model the ion exchange between the capillary wall and the BGE, which is the phenomenon determining the surface potential and hence the EOF. Several approaches relating ζ to the BGE composition have been reported [7, 15, 21–23]. Following these works, here we use and discuss a model proposed recently by the authors [7], which was initially

aimed at describing silica capillary interfaces, where the main source of surface charge is the dissociation of silanol groups. Derivations were made in the framework of Poisson–Boltzmann theory, with further considerations of surface chemistry to account for surface charge generation. In the present work we extend the model to the case of polymer capillaries, where the ionizable species are carboxylate groups.

The main aspects of the model are outlined in the next section. Then, the results of applying the model to experimental data available in the literature are shown. The data considered involve different systems for which the EOF was measured and the zeta potential was calculated through Eq. (1). Special emphasis is placed on the case of synthetic organic polymer capillaries. In this section we also include examples of silica capillaries for the purposes of visualizing the reach of the model predictions.

Theoretical concepts

In the framework of the standard electrokinetic model [24, 25], the interface composed of a solid surface in equilibrium with an aqueous electrolyte solution is shown schematically in Fig. 1. The dissociation of acid groups attached to the capillary wall generates a negatively charged surface, with charge density per unit area σ_0. The electrostatic potential associated with this charge density decreases away from the surface because of counterion screening. In particular, the region between $x=0$ and $x=d$, the compact layer, is generally assumed to be free of charges owing to the finite size of the hydrated ions. Thus the potential drop across this layer is written [4]

$$\psi_0 - \psi_d = \sigma_0 / C_{in}, \tag{2}$$

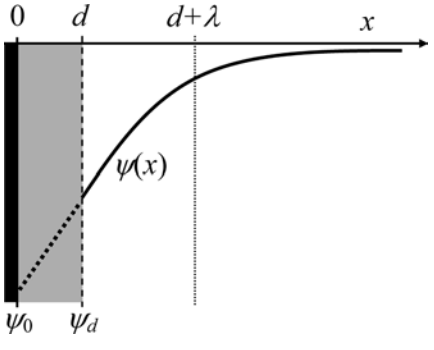

Fig. 1 Schematic representation of the electrostatic potential $\psi(x)$ in the solid–liquid interface of a capillary tube used in electrophoresis. In this scheme, $x=R-r$, where R is capillary radius and r is the radial cylindrical coordinate. Also ψ_0 is the surface potential, ψ_d is the potential at the outer Helmholtz plane, d is the thickness of the compact layer and λ is the Debye screening length. When an electrical field is applied along the capillary, normal to the x-direction, the electric force acting on the ions drags the electrolyte solution through the capillary. The limiting value of the electroosmotic velocity is given by Eq. (1), provided $\zeta \approx \psi_d$ and $\lambda << R$

where C_{in} is the capacitance per unit area of the inner region between the equipotential planes at ψ_0 and ψ_d (see also the legend to Fig. 1). For $x \geq d$, in the diffuse layer, the ion distribution is determined by the balance between entropic and electrostatic forces, and hence $\psi(x)$ is governed by the Poisson–Boltzmann equation. The characteristic screening length illustrated in Fig. 1 is $\lambda = \left(\varepsilon k_B T / e^2 \sum_k z_k^2 n_k^b\right)^{1/2}$, where e is the elementary charge, k_B is the Boltzmann constant, T is the absolute temperature, z_k are the ion valences and n_k^b are the ion number densities in the bulk. In typical conditions of CZE, λ is smaller than the capillary radius R.

The total charge density in the diffuse layer, σ_d, involves the summation over all ion species as follows:

$$\sigma_d = \left\{ 2\varepsilon k_B T \sum_k n_k^b \left[\exp\left(-\frac{e z_k \psi_d}{k_B T} \right) - 1 \right] \right\}^{1/2}. \tag{3}$$

In addition, it is assumed throughout this work that $\zeta \approx \psi_d$ (see also Refs. [4, 24, 26]). Thus Eq. (3) relates ζ to the concentration of the ions in solution. In addition, a suitable relation between the molar concentration of protons in the bulk, $[H^+]$, and the surface charge density is required. For this purpose, we consider a system composed of a solid surface containing n_s weak acid groups per unit area in equilibrium with a large electrolyte reservoir. Consequently, the equilibrium dissociation constant K_s is obtained in the framework of statistical thermodynamics [22]. Thus the charge density as a function of $[H^+]$ is found to be

$$\sigma_0 = \frac{-e n_s}{1 + ([H^+]/K_s)\exp(-e\psi_0/k_B T)}, \tag{4}$$

where en_s is the total number of surface charges per area unit available. Therefore, through the electroneutrality condition ($\sigma_d + \sigma_0 = 0$), Eqs. (2)–(4) are combined to obtain the following expression

$$\sigma_d\left(n_k^b, \zeta\right) - \frac{e n_s}{1 + 10^{(pK_s - pH)} \exp\left\{ \frac{-e}{k_B T} \left[\zeta - \frac{\sigma_d\left(n_k^b, \zeta\right)}{C_{in}} \right] \right\}} = 0, \tag{5}$$

which establishes a relationship between ζ and the BGE characteristics. Equation (5) is quite general as long as the ion densities in $\sigma_d\left(n_k^b, \zeta\right)$ are appropriately quantified through Eq. (3).

In applying the model, the first step generally consists in the evaluation of parameters n_s K_s and C_{in} from a set of N experimental data $\left\{pH, n_k^b, \zeta\right\}$. The best values of these parameters are those that minimize the sum $\sum_{i=1}^{N} (\Delta_i)^2$, where Δ_i represents the left-hand side of Eq. (5) and the subindex i refers to each triad $\left\{pH, n_k^b, \zeta\right\}$ placed into Eq. (5). Numerical calculations are carried out with a typical minimizing subroutine. Once the parameters for a given capillary are known, ζ can be predicted for a different pH and ionic strength. Thus the same numerical scheme is used, where the input data are $\left\{pH, n_k^b\right\}$ and the only unknown is ζ.

Results and discussion

In this section, before the model is used to predict the zeta potential of organic polymer capillaries, we firstly discuss some examples involving classical materials, as an illustration of the model application. In this sense, Fig. 2 shows data of ζ as a function of pH, which were obtained with a vitreous silica capillary at 25 °C. The experimental conditions are described in Ref. [21]. Also in Fig. 2, lines represent the model predictions with the parameter values reported in this figure legend. In this sense, one may observe that typical values of C_{in} are in the range

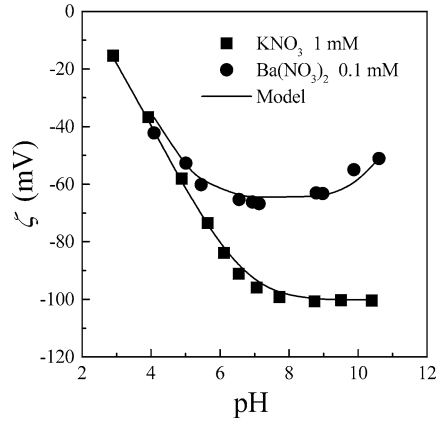

Fig. 2 Zeta potential of a vitreous silica capillary as a function of pH, for different salt solutions at 25 °C. The *symbols* are experimental data from Ref. [21]. The *lines* are the prediction of Eq. (5) with the following parameter values: for KNO_3, $pK_s = 3.5$, $C_{in} = 0.17$ F m^{-2} and $n_s = 0.8\times10^{17}$ m^{-2}; for $Ba(NO_3)_2$, $pK_s = 3.7$, $C_{in} = 0.5$ F m^{-2} and $n_s = 0.45\times10^{17}$ m^{-2}

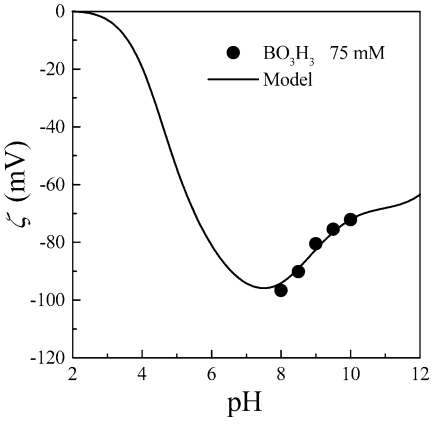

Fig. 3 Zeta potential of a fused silica capillary as a function of pH, when a buffer solution is used as the background electrolyte at 25 °C. The *symbols* are experimental data from Ref. [7]. The *lines* are the prediction of Eq. (5) with the following parameter values: $pK_s = 6$, $C_{in} = 1$ F m^{-2} and $n_s = 3.5\times10^{17}$ m^{-2}

0.1–1 F m^{-2} [4] and the number density n_s reported in the literature is around 10^{17} m^{-2} [3, 9]. On the other hand, in the case of solutions of KNO_3, the ionic strength remains almost constant since the concentration of salt (1 mM) exceeds greatly the concentration of acid or base added to adjust the pH. In contrast, the ionic strength of $Ba(NO_3)_2$ solutions changes significantly for pH > 7, owing to the contribution of $Ba(OH)_2$ added to increase the pH. In fact, we found that the minimum of the curve ζ(pH) in Fig. 2 (an experimental feature discussed in the literature [21]) is predicted well by the model when the equivalents of $Ba(OH)_2$ are considered in the evaluation of $\sigma_d\left(n_k^b, \zeta\right)$ [7].

Another example concerning a buffer solution (no added salt) is analyzed in Fig. 3. The data correspond to a fused silica capillary with a 75 mM solution of boric acid, the pK_a value of which is 9.2 at 25 °C. The experimental conditions are described in Ref. [7]. In this figure, the line represents the model prediction with the parameter values reported in the figure legend. In particular, the value of pK_s found had been previously reported elsewhere [27]. The experimental data are in the zone where boric acid has an effective buffering action. The model prediction is also shown out of this zone to observe the response of ζ as a function of pH. It is worth noting that the model predicts the point of zero charge at a pH of around 2.5, in agreement with results reported in the literature [4, 28].

In the following we apply the model to zeta potential data obtained from EOF experiments carried out with synthetic organic polymer capillaries: polyfluorocarbon (PFC), polyethylene (PE) and poly(vinyl chloride) (PVC) [29]. The experimental details are well described in Ref. [29]. Here it is relevant to mention that the BGE, which is a mixture of buffer and salt aqueous solutions, was formulated to kept the ionic strength relatively constant at 10 mM for the whole range of pH. The experimental values from PFC and PVC capillaries are presented in Fig. 4. Data from the PE capillary are not shown for the sake of clarity, as they rather superpose the PFC data. Also in Fig. 4, lines refer to the model prediction with the parameter values reported in Table 1. A remarkable agreement between theory and experiments is observed.

The values of pK_s found coincide with those reported for carboxylate groups [4, 22], being slightly higher in the case of PVC (see also Ref. [29] and references therein). In particular, the model predicts $C_{in}\to\infty$ for all these capillaries, which means that $\zeta \approx \psi_0$. This is also an

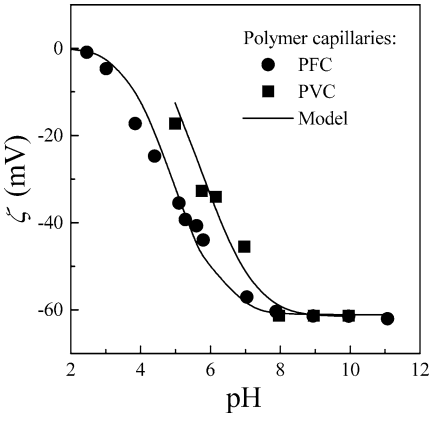

Fig. 4 Zeta potential of synthetic organic polymer capillaries [polyfluorocarbon, *PFC*, poly(vinyl chloride), *PVC*] as a function of pH at 24 °C. The *symbols* are experimental data from Ref. [29]. The *lines* are the prediction of Eq. (5) with the parameter values reported in Table 1

Table 1 Parameter values of the model applied to synthetic organic polymer capillaries, as obtained from electroosmotic flow experimental data reported in Ref. [29]

Capillary	pK_s	n_s (10^{17} m^{-2})
Polyfluorocarbon	4.55	1.09
Polyethylene	4.95	1.14
Poly(vinyl chloride)	5.50	1.10

expected result for carboxylate groups, which allow counterions to approach closely the surface and hence the compact layer thickness d is very thin [4]. For instance, values of C_{in} higher than 10^4 F m^{-2} were required in Ref. [22] to fit experimental data involving carboxylate groups attached to latex particles (see also Ref. [30] for results involving interfaces containing both carboxylate and sulfate groups). Therefore, as a result of the model, it is clear that the value of the zeta potential developed in polymeric capillaries (PFC, PVC and PE) is practically the same as that of the surface potential, which is accessible from titration experiments.

On the basis of the results discussed here, one may conclude that the model appears robust enough, in the sense that it is able to describe ζ satisfactorily for different capillary materials and BGEs within a wide range of pH and ionic strength. These calculations are thus useful to quantify and control the zeta potential in experimental programs of capillary electrophoresis.

Acknowledgements This research was supported by SEPCYT-FONCyT, PICT 09–09752, and SeCyT-UNL, CAI + D 2002, Argentina. C.L.A.B. and J.A.D. gratefully thank SECyT, CONICET, AAIFQ and the organizing committee of the 11th ICSCS for financial aid.

References

1. Dukhin SS, Derjaguin BV (1974) In: Matijevic E (ed) Surface and colloid science: electrokinetic phenomena, vol 7. Wiley, New York
2. Probstein RF (1989) Physicochemical hydrodynamics. Butterworths, New York
3. Russel WB, Saville DA, Schowalter WR (1989) Colloidal dispersions. Cambridge University Press, Cambridge
4. Hunter RJ (1992) Foundations of colloid science, vol II. Clarendon, Oxford
5. Gaš B, Štědrý M, Kenndler E (1995) J Chromatogr A 709:63
6. Griffiths SK, Nilson RH (2000) Anal Chem 72:4767
7. Berli CLA, Piaggio MV, Deiber JA (2003) Electrophoresis 24:1587
8. Grossman PD, Colburn JC (1992) Capillary electrophoresis: theory and practice. Academic, New York
9. Jandik P, Bonn G (1993) Capillary electrophoresis of small molecules and ions. VCH, New York
10. Khun R, Hoffstetter-Khun S (1993) Capillary electrophoresis: principles and practice. Springer, Berlin Heidelberg New York
11. Kenndler E (1998) Chem Anal 146:25
12. Kenndler E, Gassner B (1990) Anal Chem 62:431
13. Schwer Ch, Kenndler E (1991) Anal Chem 63:1801
14. Kenndler E, Friedl W (1992) J Chromatogr 608:161
15. Tavares MFM, McGuffin VL (1995) Anal Chem 67:3687
16. Kenndler E (1998) J Microcolumn Sep 10:273
17. Saville DA, Palusinski OA (1986) AIChE J 32:207
18. Palusinski OA, Graham A, Mosher RA, Bier M, Saville DA (1986) AIChE J 32:215
19. Reijenga JC, Kenndler E (1994) J Chromatogr A 659:403
20. Piaggio MV, Deiber JA (2003) Lat Am Appl Res 33:171
21. Wiese GR, James RO, Healy TW (1971) Discuss Faraday Soc 52:302
22. Healy TW, White LR (1978) Adv Colloid Interface Sci 9:303
23. Salomon K, Burgi DS, Helmer JC (1991) J Chromatogr 559:69
24. Dukhin SS (1995) Adv. Colloid Interface Sci 61:17
25. Dukhin SS, Zimmermann R, Werner C (2001) Colloids Surf A 195:103
26. Attard P, Antelmi D, Larson I (2000) Langmuir 16:1542
27. Hewlett-Packard (2000) Hewlett-Packard instrument guide CD-ROM, plate 010–023, CE basics. Hewlett-Packard
28. Kosmulski M (2002) J Colloid Interface Sci 253:77
29. Schützner W, Kenndler E (1992) Anal Chem 64:1991
30. Gisler T, Schultz SF, Borkovec M, Sticher H, Schurtenberger P, D'Aguanno B, Klein R (1994) J Chem Phys 101:9924